Islam M. Ibrahim[1], Nada I. Farah[2], Mohamed I. Ahmed[3], Hala M Abdelkader[4], Ahmed Jamal Abdullah Al-Gburi[5], Zahriladha Zakaria[5], Rania H. Elabd[6], M. M. Elsherbini[1,4]

Department of Electrical Engineering, The Egyptian Academy for Engineering and Advanced Technology (EAEAT) (1)
Kuwait Technical College (2)
Microstrip Department, Electronic research institute, El-Nuzha, Cairo, 11843, Egypt (3)
Department of Electrical Engineering, Shoubra Faculty of Engineering Benha University, Cairo, 11629, Egypt (4)
Center for Telecommunication Research & Innovation (CeTRI), Fakulti Teknologi dan Kejuruteraan Elektronik dan Komputer (FTKEK), Universiti Teknikal Malaysia Melaka (UTeM), Malacca, Malaysia (5)
Electronic and Communication Dept., Higher Institute of Engineering and Technology in New Damietta, Damietta 34517, Egypt (6)
ORCID: 1. 0009 – 0002 – 6965 – 5630, 2. 0009 – 0007 – 6427 – 5766, 3. 0000 – 0001 – 7485 – 9406, 4. 0000 – 0001 – 7485 – 9406, 5. 0000-0002-5305-3937, 6. 0000-0003-1467-405X, 7. 0000-0002-4468-0277, 8. 0000-0003-0083-7831

doi:10.15199/48.2024.02.03

A Composite Matrix of Mm-Wave Antenna Arrays for 5G Applications

Abstract. *This work designs, simulates, and fabricates a millimeter-wave antenna array for a 5G base station to support the significant improvements that come with the new 5G technology. The work starts with 1x8 arrays with sizes of 64.21.2 mm² and 55x20.2 mm² for 28 and 38 GHz, respectively. The elements are then increased to 8x8 arrays with dimensions of 64x169 mm² for 28 GHz and 55x161.5 mm² for 38 GHz. The proposed design is further promoted to a 16x8 array antenna with dimensions of 74x255x0.508 mm³. This antenna configuration initially consists of an 8x8 series-fed array operating at 28 GHz and another 8x8 operating at 38 GHz, all implemented on a Rogers/RT 5880 substrate with ε_r=2.2. At 28 GHz and 38 GHz, the radiation efficiency was measured to be 97.6% and 96.8%, respectively, and the greatest actual gain was 24.7 dBi. Additionally, the antenna array significantly boosts gain. The antenna's performance spans a dual-band millimeter-wave spectrum operating at 28–38 GHz. Specifically, at 28 GHz, 8x8 arrays have a realized gain of 20.33 dBi, and at 38 GHz, the gain is 22.23 dBi. Moreover, for the antenna range, the model displays a symmetrical radiation pattern, and the side lobe level is diminished to -10.2 dB. Two simulation programs, MWSCST2020, and ANSYS HFSS19, are used to simulate these array antennas. The simulation results closely match the actual model performance. Furthermore, the antenna is measured using an Agilent R&S Z67 VNA.*

Streszczenie. *W ramach tej pracy projektuje, symuluje i wytwarza układ anten wykorzystujących fale milimetrowe dla stacji bazowej 5G, aby wspierać znaczące ulepszenia wprowadzone w nowej technologii 5G. Prace rozpoczynają się od układów 1x8 o rozmiarach 64,21,2 mm² i 55x20,2 mm² odpowiednio dla 28 i 38 GHz. Elementy są następnie powiększane do macierzy 8x8 o wymiarach 64x169 mm² dla 28 GHz i 55x161,5 mm² dla 38 GHz. Proponowany projekt jest dalej promowany do anteny szeregowej 16x8 o wymiarach 74x255x0,508 mm³. Ta konfiguracja anteny początkowo składa się z układu zasilanego szeregowo 8x8 pracującego przy 28 GHz i kolejnego 8x8 pracującego przy 38 GHz, wszystkie zaimplementowane na podłożu Rogers/RT 5880 z εr=2,2. Dla częstotliwości 28 GHz i 38 GHz zmierzona efektywność promieniowania wyniosła odpowiednio 97,6% i 96,8%, a największe rzeczywiste wzmocnienie wyniosło 24,7 dBi. Dodatkowo układ anten znacznie zwiększa zysk. Wydajność anteny obejmuje dwuzakresowe widmo fal milimetrowych w paśmie 28–38 GHz. W szczególności przy 28 GHz macierze 8x8 mają zrealizowany zysk na poziomie 20,33 dBi, a przy 38 GHz zysk wynosi 22,23 dBi. Ponadto dla zasięgu anteny model wykazuje symetryczną charakterystykę promieniowania, a poziom listka bocznego jest obniżony do -10,2 dB. Do symulacji tych anten szeregowych służą dwa programy symulacyjne, MWSCST2020 i ANSYS HFSS19. Wyniki symulacji są ściśle zgodne z rzeczywistą wydajnością modelu. Ponadto antena jest mierzona za pomocą Agilent R&S Z67 VNA*. (***Złożona macierz układów anten Mm-Wave do zastosowań 5G***)

Keywords: Millimeter Wave – 5G Technology – Arrays –Gain
Słowa kluczowe: Fala milimetrowa – Technologia 5G – Macierze – Wzmocnienie

Introduction

Smart cities are an example of large-scale IoT application cases. To reduce traffic congestion, for instance, connected traffic lights use data from sensors and moving vehicles to alter the timing and cadence of their lights in real-time response to traffic. The idea of a "smart city" aims to deploy 5G millimeter-wave antennas to improve the capabilities of the city and address a variety of issues. This antenna mimics a millimeter wave quaternion MIMO 28 GHz antenna. Due to the employment of an inverted trapezoidal radiation patch and a slotted trapezoidal ground plate structure in the antenna design, it can operate in the frequency range of 24-32 GHz. The MIMO antenna's gain at 28 GHz is 7.5 dBi [1].

The frequency responses show that an axial ratio of 3 dB and VSWR of 2 are reached at a bandwidth of 21%, where the gain is greater than 13.3 dBi [2]. These two antennas show resonance at 3.5 GHz, 5.7 GHz, 7.5 GHz, and 9.3 GHz in both planar and conformal modes. The antenna parameters in the suggested models for antennas, such as gain, radiation pattern, VSWR, reflection coefficient, and gain [3]. A printed multiple-input multiple-output (MIMO) antenna with good diversity performance and straightforward geometry for fifth-generation (5G) mm-wave applications [4]. The proposed construction achieves a maximum gain of 12.02 dBi, while the proposed antenna covers the 5G mm-wave band with a 10 dB bandwidth ranging from 27.6-28.6 GHz. Additionally, the increased diversity gain, reduced channel capacity loss, and lower channel correlation values make it a strong candidate for 5G MIMO applications in the mm-wave spectrum [5].

The proposed antenna consists of circular rings stacked vertically and horizontally on top of one another on a very thin RO5880 substrate. The radiating element measures 6 x 2 x 0.254 mm3, while the single element antenna board has dimensions of 12 x 12 x 0.254 mm3. The suggested antenna displayed dual-band properties. A second resonance with a bandwidth of 3.25 GHz ranged from 37.75 to 41 GHz, respectively [6]. The proposed structure is made of a ring-shaped patch with a square slot etched at the top middle of the partial ground plane and is designed at 0.256 mm thickness. Roggers 5880. With a simulated gain of 3.95 dBi and total efficiency of 96% for a single element, a high bandwidth of 8 GHz ranging from 26 to 32 GHz is achieved by tweaking the ring and square slot characteristics. The construction is then further altered into a four-element linear array [7]. The resonant structure is created on a RO5880 substrate that is 0.254 mm thin and has a relative permittivity of 2.3. The design's single element displayed resonance behaviour between 26.5 and 41 GHz, with a peak gain of 4 dBi and a 96% radiation efficiency.

Four elements are added to the multicurricular ring antenna element to create an array system. With a peak gain of 11 dBi, the array size is kept at 18.25 12.5 0.254

mm3 [8]. The antenna simulates a 37.5 GHz to 69.5 GHz bandwidth with a 60% fractional bandwidth. The largest gain value among them for 62 GHz is 2.64 dBi. A broader bandwidth is obtained from 20.9 GHz to 67 GHz, with a fractional bandwidth of104.89%. This bandwidth includes the millimeter wave application frequencies of 28 GHz, 38 GHz, and 60 GHz [9]. A 4-port, significant isolation, and gain-enhanced multiple-input multiple-output (MIMO) antenna operating at 38 GHz is introduced. The recommended antenna element is a monopole antenna with a central frequency of 38 GHz that operates between 36.6 GHz and 39.5 GHz thanks to a partial ground plane and a circular patch with a rectangular slit cut out of it. The four elements are placed orthogonally to limit mutual coupling between them at the desired frequency ranges, and four stubs are added to increase isolation [10]. A 1x4 array model with a 20.5% impedance bandwidth (23.1–28.3 GHz) is developed and measured as evidence [11].

The creation of precoding vectors at the transmitter and vector combining at the receiver during the establishment and maintenance of directional links is a well-known issue with pencil beamforming (BF). It is made difficult by the enormous antenna array's (AA) size and the necessary channel state information (CSI) exchange, which takes a long time for the equipment used by vehicles [12]. The array arrangement achieved a measured impedance bandwidth of 29%, an axial-ration (AR) bandwidth of 13%, and a broadside gain of 13.7 dBi at 28 GHz. It was constructed well and characterized by good performance [13]. The antenna has a measured impedance bandwidth of 14.5 GHz (52% at 28 GHz) that is 10 dB wide, and it has a maximum peak realized gain of 20.44 dBi at 27.5 GHz with a 3 dB gain bandwidth of 3.5 GHz (12.5% at 28 GHz). The benefits of the proposed antenna array's simple feeding structure, wide bandwidth, high gain for 5G communication applications [14].

With coverage, spectrum efficiency, and BS density as the primary criteria of interest, this design compares the suggested deployments on both a qualitative and quantitative level by create a model that captures the details of multiple deployment alternatives [15]. A microstrip patch with a two-pronged fork-like structure is used as the only radiating element in the antenna array. The realized gain for the single radiator is 7.6 dBi. A 64-element array antenna design is suggested in order to meet the gain needed for 5G base stations, which has a bore side gain of 21.2 dBi at 37.2 GHz. 8 by 8, 8 by 16, and an 8 by 32 antenna array [16]. A dual-band, MIMO, two-element 28/38 GHz antenna is suggested for the next 5G network. A slot monopole antenna loaded with stubs and a tiny crescent with a total area of 15 mm^2 make up the single element. to increase the coupling between parts without utilizing any decoupling structures, one of the antennas is printed on the top layer while the other is placed on the substrate's back [17]. With a broad operating band in the range of 23.9–30.7 GHz, a high peak gain of 9.4 dBi, and radiation efficiency of more than 87%, the developed antenna performs much better. Based on this concept, a four-port MIMO antenna configuration. These features cover the entire global mm-wave 5G spectrum band of 24.25-29.5 GHz. [18].

A stepped line cut and U-slot combined ultra-wideband microstrip array antenna design is designed to increase bandwidth performance, The antenna design has a gain of 8.71 dB, a bandwidth of 4.47 GHz, and a frequency range of 28 GHz [19]. For the 28 GHz band, the first design is a single-element circular construction with an elliptical slot and a flawed ground structure with dimensions of 6 mm by 7 mm, symmetric two-element MIMO slotted circular patch antennas, uses dimensions of 7 mm by 6 mm. On a Rogers Duroid 5880 substrate with a relative dielectric permittivity of 2.2 and a thickness of 0.8 mm, the suggested four-port MIMO antenna is built. This proposed MIMO antenna measures 20 by 20 by 0.8 mm3 in total [20].

A director-equipped broad-band log periodic dipole antenna (LPDA) with dimensions of 20 x 40 x 0.508 mm3. The LPDA is made up of four arms with alternate stubs that are uniformly spaced on both lines. The 50- main feeder line is positioned on partially level ground near the substrate's back. In order to increase gain, further minimize side lobes, and broaden the frequency range, the directors are additionally included and examined in a regular matrix at a predetermined distance. The antenna's performance spans a large millimeter wave spectrum, from 26 to 44 GHz. At 28 GHz, 35 GHz, 38 GHz, and 43 GHz, the antenna's realized gain is 8.97, 11.96, 13.96, and 14.29 dB, respectively [21].

The work contribution consists of a composite Mm-wave antenna array model with 16x8 array elements encompassing the dual band resonant frequencies (28–38 GHz). Both single arrays at 28 GHz and 38 GHz are designed, simulated, and fabricated on the same substrate to maximize the gain, decrease mutual coupling, and improve the matching between array elements. The antenna became more efficient as well, and thanks to a decrease in SLL (side lobe levels), it currently has the highest realized gain overall. This constructed antenna serves as a base station for 5G applications. This work has a superior outcome when compared to the earlier work displayed in Table 3. The antenna configuration is simple and inexpensive in design complexity.

Antenna Design and Configuration (1x8 Series Fed Arrays)

The model designed for the Roger RT5880, which has dimensions of 64 x 21.2 mm2 at 28 GHz and a substrate thickness of 0.254 mm, a relative permittivity of 2.2, and a tangent loss of 0.0009, is shown in Figure 1 as the basic arrangement of an 8-element series-fed array. In order to match the readings from the VNA (vector network analyzer), the feeder Zo is set to be approximately 50 ohms. To satisfy the design specifications, a 28 GHz array with the greatest gain and efficiency was chosen since it had the ideal size.

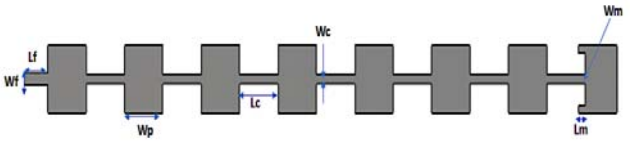

Fig.1. The geometry of the proposed 1x8 Series Fed array(28GHz). Where: $W_{P=}$ =3.53, W_c= 0.49, L_c= 3.35, W_m=2.72, L_m=0.62, W_f=2.2 and L_f=1.8. All dimensions are in mm.

8x8 Series Fed Array at 28GHz

To boost gain and directivity, an 8x8 array of elements will be built on the same material as the previously generated 1x8 array and operated at 28 GHz. The row spacing of the array is 34 inches, or 8 millimeters, from the centers of the patches.

1x8 Series Fed Array at 38GHz

Second, the proposed 1x8 array operating at 38 GHz is similar to its counterpart at 28 GHz. To attain the 38 GHz frequency, this design required numerous alterations to the parameters to reduce the length and width shown in fig. 2.

Series Fed Array at 38GHz

The 8x8 array antenna is now also intended to function at 38 GHz in order to improve gain and directivity. The array's row spacing is, measured from the center of the patches, equivalent to 5.4028 mm.

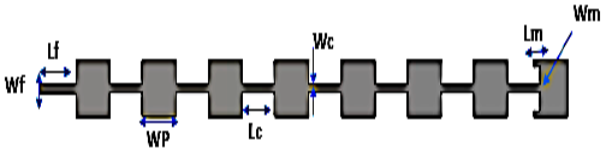

Fig.2. The geometry of the proposed 1x8 Series Fed array(38GHz). $W_{P=}$ =2.64, W_c= 2.55, L_c= 0.42, W_m=1.56, L_m=0.55, W_f=0.45 and L_f=11.57. All dimensions are in mm.

The Final Design of 16x8 Series Fed Array at 28/38GHz

A composite design with 16x8 arrays, each of which has a 1x8 series fed array, is the result of combining the 8x8 at 28 GHz and the 8x8 at 38 GHz arrays. The dimensions of each element of the arrays are 74 mm x 255 mm, the substrate height is 0.254 mm, and the material is Rogers RT5880 (lossy). The arrays are also 15 mm apart from one another to accommodate the port connection. When the port size is taken into consideration during manufacture, the connector can touch the patch, which could lead to additional radiation. The 10-mm feed line extension fixed this problem. Figure 3 shows the 16x8 series fed array antenna's built and simulated geometry.

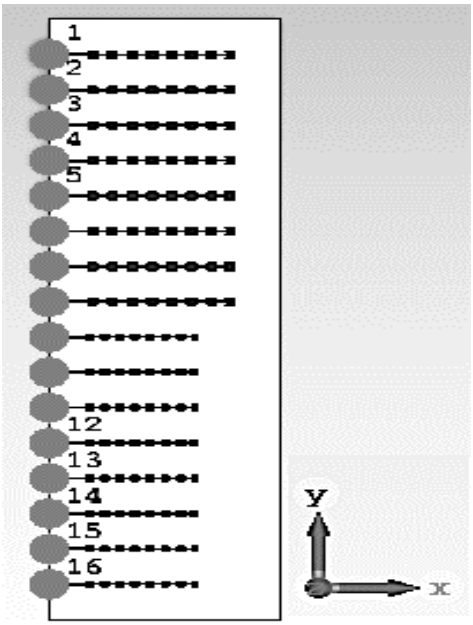

Fig.3. The Simulated geometry of the proposed 16x8 Series Fed array at (28-38GHz).

Parametric Study Results

Detailed parametric research for the gain, efficiency, and S-parameter, starting with a 1x8 array for 28 GHz and a 1x8 array for 38 GHz, up to a 16x8 array for 28–38 GHz, determined that the gain in the antenna's range simply grows with the number of array elements. The gain for a 1x8 series fed array is 15.9 at 28 GHz and 15.3 at 38 GHz, increasing the total realized gain up to 24.6 dB. Additionally, as shown in figure 4(a), the gain begins at 21.3 GHz for an 8x8 series-fed array and 20.7 GHz for an 8x8 array.

The expanded array elements demonstrate that the proposed array antenna's side lobes are directed toward the array elements with the best-optimized value. In figure 4(b), there are 97.5% efficiency tents. The array antenna's performance was improved by The MWSCST program was used to conduct numerous parametric tests to examine the impacts of a key parameter on gain, bandwidth, SLL, and efficiency. Other variables can be improved and prepared for better matching bandwidth and high gain by employing built-in optimization algorithms within the MWSCST.

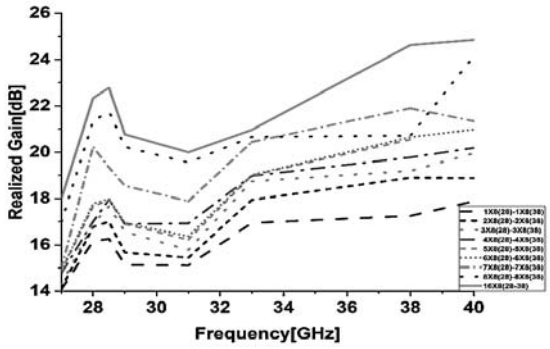

(a)

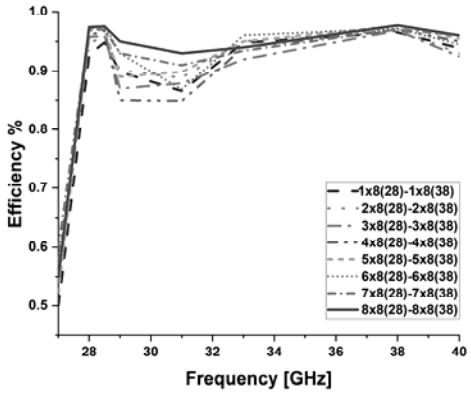

(b)

Fig.4. (a) Realized study for antenna arrays elements at 28/38GHz, (b) Radiation efficiency by increasing antenna arrays elements at 28/38GHz

Results and Discussions

Figure 5(a) shows the design return loss for 1x8 array elements at 28 GHz using MWSCST and ANSYS HFSS simulations. It is demonstrated that the S11 value using the CST simulator is -22.7 dB at 28.13 GHz. It is shown that the S11 value using the CST simulator is -22.7 dB at 28.13 GHz, whereas the S11 using HFSS has a value of -14.9 dB. Losses dropped, and the S11 value was -25 dB and -28.6 dB when another simulator was used at the same frequency of 28.13 GHz in comparison to the return loss values for 8x8 array elements in figure 5(b).

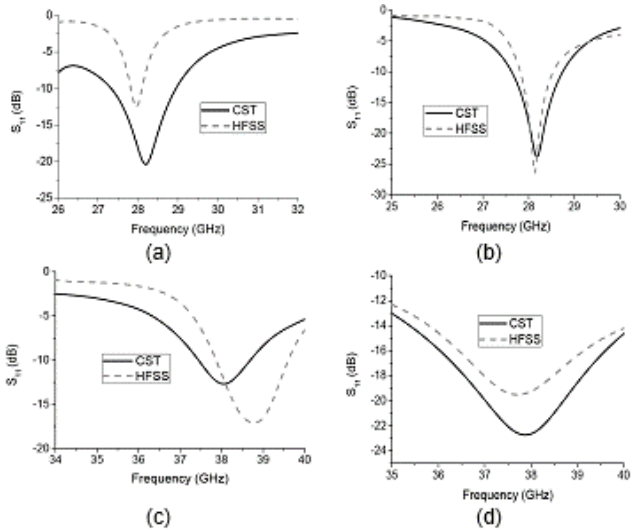

Fig. 5. (a) S11 for 1x8 Array Elements at 28 GHz, (b) S11 for 8x8 Array Elements at 28GHz, (c) S11 for 1x8 Array Elements at 38 GHz, (d) S11 for 8x8 Array Elements at 38GHz.

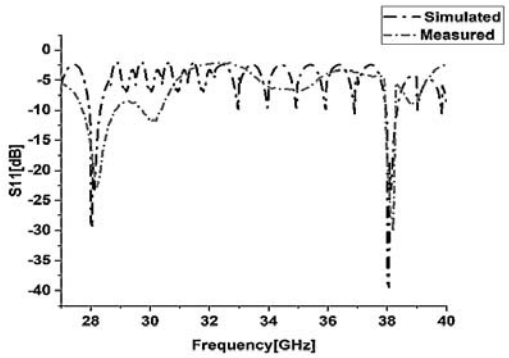

Fig.6. Measured and Simulated S11 for the proposed 16x8 Series Fed Array.

The S- parameters for 1x8 array elements at 38 GHz are presented in graph 5. (c), with a value of -14.9 dB, and for 8x8 elements at 38 GHz, is -23.89 dB, as shown in figure 5(d). This shows that the mutual coupling for the increased number of array elements caused a change in the S-parameter values, but that it had no effect on matching, and the losses were reduced by studying the parameters for the array elements' spacing in order to reduce the array coupling and prevent matching and S11 from being impacted. The return loss for 16x8 Array elements for both 28-38 GHz measured and simulated is shown in Figure 6 and S11 is -28.8 dB at 28 GHz and -40 dB at 38GHz.in Figure 6 and S11 is -28.8 dB at 28 GHz and -40 dB at 38GHz

Radiation Pattern and Gain Measurements

The antenna being tested (AUT) was not covered with any absorbent material before testing. Figures 7 and 8 depict the antenna's estimated radiation patterns in the E- and H-planes at 28 and 38 GHz, respectively. It is clear that the suggested antenna generates a stable radiation pattern throughout the stated bandwidth. The radiation patterns in the H-plane and E-plane, where the proposed antenna shows greater side-lobe suppression, utilizing observations of the radiation pattern, the gain of the antenna was estimated.

The gain was calculated using two sequential and equivalent horn antennas that were placed in a line-of-sight-aligning arrangement at a spacing of R. The first is used for broadcasting, and the second is used for receiving. Pt and Pr, respectively, stand for power sent and received. The findings of simulation and measurement show greater agreement between the simulated and measured gains shown in figure 9. The S11 in Figure 10 represents the observed return loss from the VNA because the two antennas are comparable. According to calculations, the antenna's total gain is 24.7 GHz at 38 GHz and 22.6 dBi at 28 GHz in Table 1.

Since the measurement equipment's accuracy decreases with frequency, there is a discrepancy between what was predicted and what was actually observed. This is also influenced by environmental scattering and reflection. The Performance Characteristics of the 1x8 Series fed, 8x8 Series fed, and 16x8 Series fed arrays 16X8 Series fed array is depicted in Table 2. Figure 11 is the constructed and fabricated base station model for 16x8 array elements operating between 28 and 38 GHz. The comparison between the presented array antenna and the previous work is summarized in Table 3. It shows that the proposed antenna successfully operated at two main frequencies, which are 28 GHz and 38 GHz, and achieved a high gain of 24.7 and 22.6, respectively.

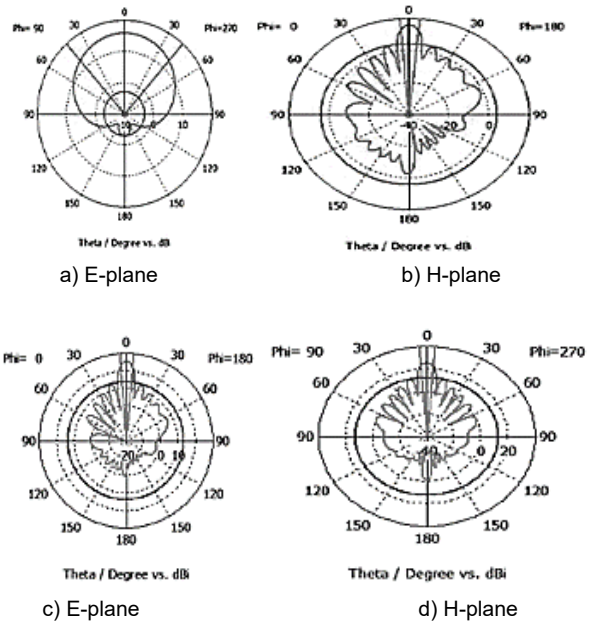

a) E-plane b) H-plane

c) E-plane d) H-plane

Fig.7. (a) The radiation pattern for 1x8 Series Fed Array at 28GHz in both E-plane and H-plane (b) The radiation pattern for 8x8 Series Fed Array at 28GHz in both H-plane.

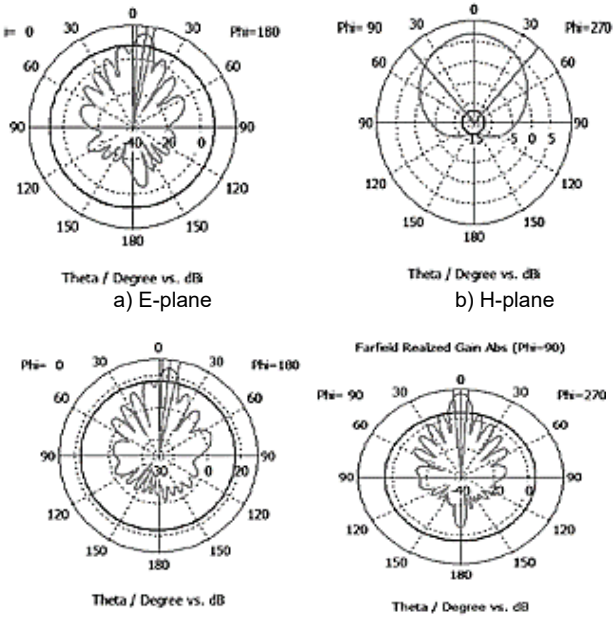

a) E-plane b) H-plane

c) E-plane d) H-plane

Fig.8. (a) The radiation pattern for 1x8 Series Fed Array at 28GHz in both E-plane and H-plane (b) The radiation pattern for 8x8 Series Fed Array at 28GHz in both H-plane.

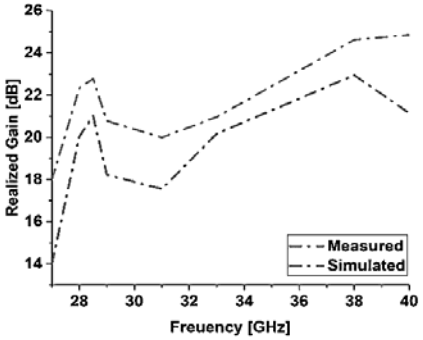

Fig.9. The total realized gain, measured and simulated.

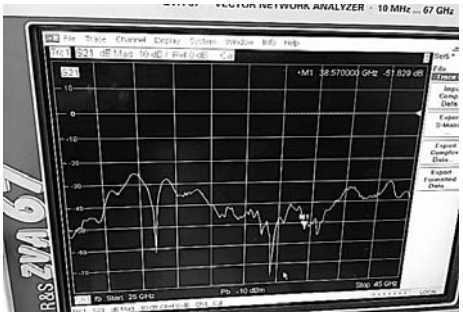

Fig.10. VNA Measured S-parameter for practical 16x8 Array at 28-38 GHz

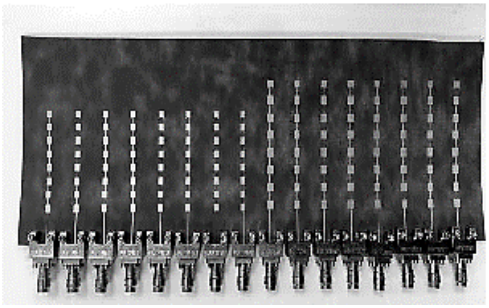

Fig.11. Base station Fabricated Model (28-38 GHz).

Table 1. Simulated and Measured 16x8 antenna array realized gain.

Frequencies [GHz]	Simulated Gain (16x8 array) [dBi]	Measured Gain (16x8 array) [dBi]
28	22.6	20.97
38	24.7	22.89

Table 2. The Performance Characteristics of the 1x8 Series fed, 8X8 Series fed and 16X8 Series fed Array

Parameter	1x8 series fed array	1x8 series fed array	8x8 series fed array	8x8 series fed array	16x8 series fed array
Resonant frequency	28	38	28	38	28-38
Size	64x21.2	55x20.2	64x169	55x161.5	74x255
S_{11} (dB)	-22.7	-14.9	-25	-23.89	-28.5/-39.1
Gain(dB)	15.9	15.3	21.3	20.7	24.7-22
Rad. Eff. (%)	94.2	95	93.2	94	96.2-97.6
Total Eff. (%)	93.78	94.8	93	92	97.6-96.8
HPBW (degree)	83.1	83.7	8.5	10.2	12.8-14.3
Side Lobe Power (dB)	-18.8	-18.7	-13	-7.4	-10.2/-6.6

Table 3. Comparison Between Presented Array Antenna and The Previous Work

Ref. No.	Resonant Freq. (GHz)	S_{11} (dB)	Realized Gain (dBi)	Rad. efficiency (%)	Design Complexity	Fabrication technology	Array elements
[32]	28-38.5	-36.6	9,10.3	95.6	Complex	PCB	1x4
[33]	28.2	-25.45	11.26	95.42	Simple	PCB	single
[34]	28	-32.3	12.15	91.5	Medium	PCB	2x2
[35]	28.83-38.96	-30, -40	16.52, 15.35	-	Complex	PCB	32
[36]	37.2	-30	21.2	92.6	Complex	PCB	1x8,8x8,16x8
[37]	28	-19.5	10.2	94	Medium	PCB	1x8
[38]	28-38	-25	5.7, 6.9	86	Medium	PCB	2x2
[39]	31 -41.5	-34.88	15	95.6	Complex	PCB	1x8
[40]	28-38	-36.6	7.9,13.4	85.5	Medium	PCB	2x4
Propoesd work	28-38	-28.8, -39.1	24.7, 22.6	96.2, 97.6	Simple	PCB	1x8,8x8,16x8

Conclusion

One of the ideal designs for smart cities is an antenna that operates in the 5G band of communications. According to this design, technology can enhance people's quality of life by yielding intelligent outcomes. In this paper, the design has been proposed to operate in the 28-38 dual-band. This design is an 8x8 series-fed antenna array for 28 GHz and another one for 38 GHz to be put together in the form of a 16x8 array, which enriches the gain, increases the antenna efficiency, and reduces the side lobe levels. Desirable results have been obtained from the proposed design. The return loss S11 is reached at -28.8 dB at 28 GHz with 5.4% bandwidth and -39.1 dB at 38 GHz with 3.1% bandwidth, and the simulated radiation pattern illustrates a maximum gain of 24.7 dBi at 28 GHz and 22.6 dBi at 38 GHz. The radiation efficiency is 97.6% and the total efficiency is 96.8%. The side lobe level was reduced to -10.2 dB. This proposed array antenna is simulated using MWSCST 2020 and HFSS 15. also measured by R&S Z67VNA. The antenna is one of the possible possibilities for usage in 5G applications since it has greater qualities than the existing antenna described in the literature, according to simulation and measurement data.

ACKNOWLEDGMENTS *The authors would like to thank and acknowledge the support provided by Universiti Teknikal Malaysia Melaka (UTeM) and the Malaysian Ministry of Higher Education (MOHE).*

The correspondence address is: Zahriladha Zakaria, Center for Telecommunication Research & Innovation (CeTRI), Fakulti Teknologi dan Kejuruteraan Elektronik dan Komputer (FTKEK), Universiti Teknikal Malaysia Melaka (UTeM), Malacca, Malaysia. E-mail: zahriladha@utem.edu.my

REFERENCES

[1] Ali, W., Das, S., Medkour, H., & Lakrit, S. (2023). Planar dual-band 27/39 GHz millimeter-wave MIMO antenna for 5G applications. Microsystem Technologies, 27, 283-292. http://doi.org.10.2528/PIERL22101702.

[2] Hirose, K., Tamura, Y., Tsugane, M., & Nakano, H.2022 Coplanar Series-Fed Spiral Antenna Arrays for Enlarged Axial Ratio Bandwidth. http://doi.org/10.2528/PIERL22100901.

[3] Praveena Kati and Venkata Kishore Kothapudi , "High-Isolation and Side Lobe Level Reduction for Dual-Band Series-Fed Centre-Fed X/Ku Shared Aperture Binomial Array Antenna for Airborne Synthetic Aperture Radar Applications," Progress In Electromagnetics Research B, Vol. 101, 175-191, 2023.
[4] Rania Hamdy Elabd, Ahmed Jamal Abdullah Al-Gburi, SAR assessment of miniaturized wideband MIMO antenna structure for millimeter wave 5G smartphones, *Microelectronic Engineering*,Volume 282,2023,112098.
[5] Munir, M. E., Kiani, S. H., Savci, H. S., Marey, M., Khan, J., Mostafa, H., & Parchin, N. O. (2023). A Four Element Mm-Wave MIMO Antenna System with Wide-Band and High Isolation Characteristics for 5G Applications. Micromachines, 14(4), 776. https://doi.org/10.3390/mi14040776.
[6] Kamal, M. M., Yang, S., Kiani, S. H., Anjum, M. R., Alibakhshikenari, M., Arain, Z. A., Limiti, E. (2021). Donut-shaped mmWave printed antenna array for 5G technology. Electronics, 10(12), 1415.
[7] Swetha Velicheti Santosh Pavada Prudhivi Mallikarjuna Rao and Mosa Satya Anuradha , "Design of Conformal Log Periodic Dipole Array Antennas Using Different Shapes of Top Loadings," Progress In Electromagnetics Research M, Vol. 116, 91-102, 2023.
[8] Chung, M. A., Chen, Y. H., & Meiy, I. P. (2023, February). Antenna-on-Chip for Millimeter Wave Applications Using CMOS Process Technology. In Telecom (Vol. 4, No. 1, pp. 146-164). MDPI. https://doi.org/10.3390/telecom4010010.
[9] A. J. A. Al-Gburi, Z. Zakaria, I. M. Ibrahim, and E. Bt A. Halim, "Microstrip patch antenna arrays design for 5G wireless backhaul application at 3.5 GHz," *Lecture Notes in Electrical Engineering, Springer Singapore*, 2022, pp. 77–88, doi: 10.1007/978-981-16-9781-4_9.
[10] Feng, S., Xin, X., & Chuxuan, R. (2022). 5G Millimeter Wave Endfire Array Antenna with Printed Inverted-F Structure. International Journal of Antennas and Propagation, 2022. https://doi.org/10.1155/2022/8940715.
[11] Fokin, G., & Volgushev, D. (2023). Model for Interference Evaluation in 5G Millimeter-Wave Ultra-Dense Network with Location-Aware Beamforming. Information, 14(1), 40. https://doi.org/10.3390/info14010040.
[12] Abdou, T. S., Saad, R., & Khamas, S. K. (2023). A Circularly Polarized mmWave Dielectric-Resonator-Antenna Array for Off-Body Communications. Applied Sciences, 13(3), 2002. https://doi.org/10.3390/app13032002.
[13] Chen, Z., Zhang, W., & Wang, K. (2023). Single-Layer Interconnected Magneto-Electric Dipole Antenna Array for 5G Communication Applications. Electronics, 12(4), 922. https://doi.org/10.3390/electronics12040922.
[14] Al-Gburi, A.J.A., Zakaria, Z., Ibrahim, I.M., Halim, E.B.A. (2022). Microstrip Patch Antenna Arrays Design for 5G Wireless Backhaul Application at 3.5 GHz. In: Zakaria, Z., Emamian, S.S. (eds) Recent Advances in Electrical and Electronic Engineering and Computer Science. Lecture Notes in Electrical Engineering, vol 865. Springer, Singapore. https://doi.org/10.1007/978-981-16-9781-4_9.
[15] Al-Gburi, A.J.A.; Ibrahim, I.M.; Zakaria, Z.; Nazli, N.F.M. Wideband Microstrip Patch Antenna for Sub 6 GHz and 5G Applications. *Przegląd Elektrotechniczny*. 2021, 11, 26–29.
[16] Ali, W. A., Ibrahim, A. A., & Ahmed, A. E. (2023). Dual-Band Millimeter Wave 2× 2 MIMO Slot Antenna with Low Mutual Coupling for 5G Networks. *Wireless Personal Communications*, 1-18. https://doi.org/10.1007/s11277-023-10267-w.
[17] Cao, T. N., Nguyen, M. T., Phan, H. L., Nguyen, D. D., Vu, D. L., Nguyen, T. Q. H., & Kim, J. M. (2023). Millimeter-Wave Broadband MIMO Antenna Using Metasurfaces for 5G Cellular Networks. International Journal of RF and Microwave Computer-Aided Engineering, 2023. https://doi.org/10.1155/2023/9938824.
[18] C. R. Jetti et al., "Design and Analysis of Modified U-Shaped Four Element MIMO Antenna for Dual-Band 5G Millimeter Wave Applications," Micromachines, vol. 14, no. 8, p. 1545, Jul. 2023, doi: 10.3390/mi14081545.
[19] Ibrahim, I. M., Ahmed, M. I., Abdelkader, H. M., & Elsherbini, M. M. (2022). A Novel Compact High Gain Wide-Band Log Periodic Dipole Array Antenna for Wireless Communication Systems. Journal of Infrared, Millimeter, and Terahertz Waves, 1-23. https://doi.org/10.1007/s10762-022-00891-1.
[20] Ikram, M., Sultan, K. S., Abbosh, A. M., & Nguyen-Trong, N. (2022). Sub-6 GHz and mm-Wave 5G Vehicle-to-Everything (5G-V2X) MIMO Antenna Array. IEEE Access, 10, 49688-49695. https://doi.org/10.1109/ACCESS.2022.3172931.
[21] Singh, M., Singh, S., & Islam, M. T. (2022). CSRR loaded high gained 28/38GHz printed MIMO patch antenna array for 5G millimeter wave wireless devices. Microelectronic Engineering, 262, 111829. https://doi.org/10.1016/j.mee.2022.111829.
[22] Munir, M. E., Al Harbi, A. G., Kiani, S. H., Marey, M., Parchin, N. O., Khan, J., ... & Abd-Alhameed, R. A. (2022). A new mm-wave antenna array with wideband characteristics for next generation communication systems. Electronics, 11(10), 1560. https://doi.org/10.3390/electronics11101560.
[23] A. J. A. Al-Gburi, I. B. M. Ibrahim, M. Y. Zeain and Z. Zakaria, "Compact Size and High Gain of CPW-Fed UWB Strawberry Artistic Shaped Printed Monopole Antennas Using FSS Single Layer Reflector," in *IEEE Access*, vol. 8, pp. 92697-92707, 2020, doi: 10.1109/ACCESS.2020.2995069.
[24] Shareef, O. A., Sabaawi, A. M. A., Muttair, K. S., Mosleh, M. F., & Almashhdany, M. B. (2022). Design of multi-band millimeter wave antenna for 5G smartphones. Indonesian Journal of Electrical Engineering and Computer Science, 25(1), 382-387. https://doi.org/10.11591/ijeecs.v25.i1.pp382-387.
[25] A. Ali et al., "A Compact MIMO Multiband Antenna for 5G/WLAN/WIFI-6 Devices," *Micromachines*, vol. 14, no. 6, p. 1153, May 2023, doi: 10.3390/mi14061153.
[26] T. Saeidi, A. J. A. Al-Gburi, and S. Karamzadeh, "A Miniaturized Full-Ground Dual-Band MIMO Spiral Button Wearable Antenna for 5G and Sub-6 GHz Communications," *Sensors*, vol. 23, no. 4, p. 1997, Feb. 2023, doi: 10.3390/s23041997.
[27] A. Khabba et al., "A new miniaturized wideband self-isolated two-port MIMO antenna for 5G millimeter-wave applications", *TELKOMNIKA Telecommunication Computing Electronics and Control*, vol. 21, no. 3, pp. 630-630, Feb. 2023.
[28] Shehata, R. E. A., Elboushi, A., Hindy, M., & Elmekati, H. (2022). Metamaterial inspired LPDA MIMO array for upper band 5G applications. International Journal of RF and Microwave Computer-Aided Engineering, 32(8), e23212. https://doi.org/10.1002/mmce.23212.
[29] Xue, H., Shen, Z., Wu, L., Rong, Y., & Peng, S. (2023). A low-profile planar end-fire broadband antenna with wide beamwidth. IET Microwaves, Antennas & Propagation. https://doi.org/10.1049/mia2.12346.
[30] Wang, X., Cao, H. R., Yan, Y. M., Yang, X. H., Zong, Z. Y., & Wu, W. (2023). Design of broadband dual-polarized reconfigurable frequency selective surface based on dual-branch parallel circuit model. IET Microwaves, Antennas & Propagation. https://doi.org/10.1049/mia2.12356.
[31] Tanabe, M., & Nakano, H. (2023). A low-profile wideband spiral antenna with multiple stopbands. IET Microwaves, Antennas & Propagation. https://doi.org/10.1049/mia2.12351.
[32] Hwang, I.J., Oh, J.I., Jo, H.W., Kim, K.S., Yu, J.W. and Lee, D.J., 2021. 28 GHz and 38 GHz dual-band vertically stacked dipole antennas on flexible liquid crystal polymer substrates for millimeter-wave 5G cellular handsets. IEEE Transactions on Antennas and Propagation, 70(5), pp.3223-3236. http://doi.org/10.1109/tap.2021.3137234..
[33] Nahas, M., 2022. A Super High Gain L-Slotted Microstrip Patch Antenna For 5G Mobile Systems Operating at 26 and 28 GHz. Engineering, Technology & Applied Science Research, 12(1), pp.8053-8057. https://doi.org/10.48084/etasr.4657.
[34] Chen, Z., Zhang, W. and Wang, K.X., 2023. A multi-port interconnected magneto-electric dipole antenna array for 5G applications. Authorea Preprints. https://doi.org/10.1049/ell2.12742.
[35] El Halaoui, M., Canale, L., Asselman, A., & Zissis, G. (2020, December). Dual-Band 28/38 GHz Inverted-F Array Antenna for Fifth Generation Mobile Applications. In Proceedings (Vol. 63, No. 1, p. 53). MDPI. https://doi.org/10.3390/proceedings2020063053.
[36] Sehrai, D. A., Khan, J., Abdullah, M., Asif, M., Alibakhshikenari, M., Virdee, B., & Falcone, F. (2023). Design of high gain base station antenna array for mm-wave cellular communication systems. Scientific Reports, 13(1), 4907. https://doi.org/10.1038/s41598-023-31728-z.
[37] Joseph, S. D., & Ball, E. A. (2023). Series-Fed Millimeter-Wave Antenna Array Based on Microstrip Line Structure. IEEE Open Journal of Antennas and Propagation, 4, 254-261. https://doi.org/10.1109/OJAP.2023.3248610.
[38] Ali, W.A.E., Ibrahim, A.A. & Ahmed, A.E. Dual-Band Millimeter Wave 2 × 2 MIMO Slot Antenna with Low Mutual Coupling for 5G Networks. Wireless Pers Commun 129, 2959–2976 (2023). https://doi.org/10.1007/s11277-023-10267-w.
[39] Yanzhi, F, Yixiang, L, &Changda, S. (2023). A Low Cross-Polarization Microstrip Antenna Array for Millimeter Wave Applications. International Journal of Antenna and Propagation, 7622014, https://doi.org/10.1155/2023/7622014.
[40] Aghoutane, B., Das, S., Ghzaoui, M.E., Madhav, B.T.P. and El Faylali, H., 2022. A novel dual band high gain 4-port millimeter wave MIMO antenna array for 28/37 GHz 5G applications. AEU-International Journal of Electronics and Communications, 145, p.154071. https://doi.org/10.1016/j.aeue.2021.154071.